

Total cross sections, hadronic geometry, and interaction dynamics in high-energy collisions

M. Buenerd and C. Furget

Institut des Sciences Nucléaires de Grenoble, 53 avenue des Martyrs, 38026 Grenoble, CEDEX, France

(Received 31 October 1988)

The geometrical interpretation of high-energy hadronic cross sections is discussed. Evidence is provided, by means of a simple model, that hadron-hadron total cross sections are not governed by geometry only, and that the interaction dynamics is flavor dependent and determines to a large extent the cross section of hadronic systems. The same conclusion is reached in a numerical approach of the problem.

I. INTRODUCTION

The total collision cross section σ_t between composite hadronic systems is a fundamental observable of the interaction process. Its particular importance relies on its relationship with the forward-scattering amplitude via the optical theorem. This confers on σ_t the status of both an integral and a differential quantity: the first as a sum of single-channel cross sections over all the open channels, the second as the imaginary part of the forward-scattering amplitude. The knowledge of σ_t constitutes a first insight into the bulk features of the interaction. It brings about first indications on the dynamics and spatial extent of the collision, although these two aspects can be really separated only when elastic differential cross sections are available. This general feature holds in various domains of hadron physics, for nuclear collisions as well as for collisions between more elementary hadrons.

Experimentally, σ_t is obtained by the attenuation method or by extrapolation of small-angle elastic-scattering measurements in fixed-target experiments and in collider experiments. For short-lived particles, the photoproduction of vector mesons constitutes a unique source of data on meson-nucleon systems. In this case however, σ_t values rely on the validity of the vector-dominance model (VDM). Note also that the double production of vector mesons in lepton collisions is another potential source of data on meson-meson systems, also relying on the VDM. However, the currently available data on these latter systems are still limited to rather small values of center-of-mass energy ($\sqrt{s} < 3$ GeV).

To introduce the issue, it is interesting to note that, for the various systems for which σ_t has been measured at $\sqrt{s} \sim 16$ GeV, the experimental values extend over a range of more than 1 order of magnitude:¹ at the upper limit of this range, one finds σ_{pp} (and $\sigma_{\bar{p}p}$) at about 40 mb, whereas at the other end, the $J/\psi p$ cross section amounts only to about 2 mb. This observation raises the question as to what is the origin of this considerable difference between elementary hadron cross sections: does it lie in the dynamics of the interaction or in the geometrical properties of the interacting hadrons?

Let us observe first that, when the scattering process is dominated by strong absorption, the colliding objects behave as black spheres, the total cross section is then governed by the geometry of the objects, and varies approximately as the square sum of their radii, i.e., $\sigma_r \approx \pi(R_1 + R_2)^2$. This situation is systematically observed in nucleus-nucleus and nucleon-nucleus collisions.^{2,3} Another characteristic feature of strong absorption is the diffractive angular distribution of the elastic scattering. It has long been recognized that the pp diffractive elastic scattering of high-energy hadrons is generated by the shadow of inelastic processes.⁴ Thus the total cross section σ_t is largely governed by the opacity of the system, and, as long as this opacity is large, σ_t should exhibit the kind of geometrical dependence quoted above. When the objects are transparent to each other, one may expect that σ_t will be proportional to the (combinatorial) number of elementary interactions between the constituents of the two systems, and we shall see below that in this case, the dependence on the geometry vanishes. This latter situation corresponds to the additive-quark-model (AQM) assumption. Such a situation is commonly encountered in elementary hadron physics where the AQM is widely applied, it is never observed in nuclear physics where the interacting systems are always dominated by a strong opacity. Coming back to the experimental values quoted above, for the pp system, the value is close to the geometrical limit as it can be estimated from the experimental (electromagnetic) size of the nucleon, whereas for $J/\psi p$, the value is much smaller than any geometrical limit estimated on similar grounds (and assuming the interaction dynamics to be the same, at the constituent level, as for pp scattering). Thus, in $J/\psi p$, the hadrons are probably more transparent to each other than in pp or $\bar{p}p$ systems. Therefore, the dynamics of the interaction at the constituent level could be quite different in the two systems. It is demonstrated in the following that these qualitative considerations find some grounds in a quantitative analysis of the data.

A recent publication¹ has investigated this problem and concludes that elementary hadron cross sections are all governed by the geometry of the hadrons. The purpose of this paper is to investigate this same issue in con-

nection with the interpretation given in Ref. 1. It addresses the same problem, but the present analysis leads to the conclusion that total cross sections cannot be governed by the geometry of the hadrons only, and that the dynamical (microscopic) part of the interaction is flavor dependent and plays a dominant role in the determination of the cross section. In Sec. II we derive a simple analytical approach of σ_t . Although the usefulness of such a toy model is mostly pedagogical, it will allow us to evaluate the geometry-dependent and geometry-independent (which we shall refer to as dynamical) part of σ_t , and to put into light the dominant role played by the latter. Note that the distinction between these two contributions is rather formal for it will be shown below that they have the same microscopic origin. It will be shown that the model is reasonably consistent with the data for light-quark (u, d) hadronic systems. Section III is devoted to a numerical approach of the same issue, which parallels that followed in Sec. II, but which uses more realistic hadronic form factors. There, we will test the ability of the approach to reproduce consistently hadronic differential cross sections, and we will see that the results obtained for σ_t are fully consistent with those obtained in the analytic approach. The conclusion is given in Sec. IV.

II. THEORETICAL FRAMEWORK AND ANALYTIC MODEL FOR TOTAL CROSS SECTIONS

The eikonal approximation and the impact-parameter representation of the scattering amplitude provide a convenient framework for the description of the scattering process. In the present work we use the approach of Ref. 5, where the invariant amplitude is given by the usual integral over the impact parameter:

$$F(t) = i \int_0^\infty b db J_0(b\sqrt{-t}) (1 - e^{-\chi(b)}), \quad (1)$$

where the complex eikonal function $\chi(b)$ results from the double folding of the hadron form factors with an effective interaction between the constituent of the interacting hadrons. It can be expressed as the Fourier transform:

$$\chi(b) = \frac{A_1 A_2}{2\pi i} \int_0^\infty d^2\mathbf{q} e^{i\mathbf{q}\cdot\mathbf{b}} G_1(t) G_2(t) f(t), \quad (2)$$

where A_i are the number of elementary constituents in the hadrons, G_i are the hadron form factors, and $t = -q^2$ is the squared four-momentum transferred in the reaction. This model allows us to separate conveniently the geometrical contribution from the dynamical part of the amplitude. In the constituent-quark-model interpretation, A_i are the number of constituent quarks of the two hadrons, and $f(t)$ is an effective constituent-constituent interaction. It contains the long-range quark-quark interaction (not perturbatively calculable from first principles at small- t values) between the valence quarks of the two hadrons, "dressed" with the contributions of the other partons in the hadrons (quarks of the sea, gluons) to the scattering process, and with multiple-scattering effects. This effective amplitude collects all the dynamical

part of the interaction.

Under the assumption of constant isotropic $f(q)$, $\chi(b)$ reduces to the form used in Ref. 1, i.e., in the configuration space

$$\chi(b) = g \int d^2\mathbf{s} T_1(\mathbf{b}-\mathbf{s}) T_2(\mathbf{s}), \quad (3)$$

where $T_i(s) = \int dz \rho_i(s, z)$ are the opacities of the colliding hadrons of densities $\rho_i(r)$, and where g will be discussed below.

In relations (1) and (2), the scattering amplitude, and ultimately the total cross section, are governed by the eikonal function $\chi(b)$: in the integral (1), a strong qq interaction will result in a modulus of the profile function $|\Gamma(b)| = |1 - e^{-\chi(b)}|$, close to unity up to a value of b determined by the spatial extent of the hadron form factors in relations (2) and (3). This corresponds to the strong-absorption situation mentioned previously. On the other hand, if the qq interaction is small enough to allow $|\Gamma(b)| \ll 1$ around $b=0$, the collision will become transparent and the dependence of the cross section on the hadron sizes will be different. This interplay between geometry and interaction strength in the colliding systems is well illustrated in (light) nucleus-nucleus collisions where the bulk of the reaction cross section is determined by geometry, whereas the (energy-dependent) elementary nucleon-nucleon cross section⁶ governs the absorption in the surface region and modulates the surface transparency.

For Gaussian densities normalized to a volume integral unity, i.e., $\rho_i(r) = (2\pi a_i^2)^{-3/2} e^{-r^2/2a_i^2}$, the corresponding opacities are $T_i(b) = e^{-b^2/2a_i^2}/2\pi a_i^2$. Using these shapes the folding integral (2) is analytic. The optical theorem and the integral (1) which can also be performed analytically² lead to the following expression for the total cross section:

$$\sigma_t = 4\pi(a_1^2 + a_2^2) [\ln(\xi) + \text{Ei}(\xi) + \gamma] \quad (4)$$

with

$$\xi = \frac{A_1 A_2}{a_1^2 + a_2^2} \frac{\sigma_0}{4\pi} \quad \text{and} \quad \sigma_0 = 4\pi \text{Im}f(0),$$

where $\text{Ei}(\xi)$ is the exponential integral⁷ and γ the Euler constant, σ_0 is an effective elementary-constituent cross section. In relation (4), the first factor is purely geometrical, whereas the second one contains both a dynamical and a geometrical dependence. The geometrical dependence in the second factor comes through the normalization condition on the densities; it stems from the fact that smaller a_i are associated with larger local densities, and then lead to a larger local opacity.

If several species of quarks with different interactions are involved in the collision, the latter relation generalizes to

$$\xi = \frac{1}{a_1^2 + a_2^2} \sum_i \alpha_i \text{Im}f_i(0) \quad \text{with} \quad \sum_i \alpha_i = A_1 A_2,$$

where α_i is the combinatorial number of quark pairs interacting with the amplitude f_i . In the following, for light-quark (u, d) systems, we have assumed two elemen-

tary amplitudes: $f_{\bar{q}q}$ for a quark-antiquark pair, and $f_{q'q}$ for any other pair with $q' \neq \bar{q}$, in order to take into account the strong-absorption effect in the annihilation channel for the former amplitude.

Let us now examine the extreme situations in this model. When the absorption is strong, i.e., when σ_0 , and then ξ , is large, relation (4) reduces to

$$\sigma_t = 4\pi(a_1^2 + a_2^2)\ln(\xi) .$$

In this case, σ_t does exhibit a dependence on the hadron geometry (reminiscent to that usually observed in nuclear collisions^{2,3}), it does not reach an asymptotic geometrical limit (because of the assumed Gaussian shapes for the densities), and grows logarithmically with the elementary interaction strength, and with the number of elementary interactions. This latter feature is at variance with the AQM assumption. Therefore, relation (4) leads to the conclusion that in the case of extremely strong absorption (such as in nuclear-type systems), the total cross section would be dominated by the hadron geometry.

The opposite extreme situation is the weak-absorption limit, corresponding to small values of σ_0 . Then the second factor in relation (4) reduces to ξ to the leading order,⁷ and one gets

$$\sigma_t = A_1 A_2 \sigma_0 ,$$

i.e., the AQM prediction. Therefore, when the system becomes transparent, σ_t does not depend anymore on the hadron geometry. Here, it is important to note, and easy to verify, that for a given value of σ_0 , the total cross section tends to a finite limit when the size of one of the hadrons tends to zero.

The above results are in sharp contradiction with the geometrical dependence predicted in Ref. 1 for the total cross section, i.e., $\sigma_t \approx a_1^2 a_2^2$, with $a_i^2 = \langle r_i^2 \rangle / 3$, r_i being the mean-square radii of the hadrons. The reason for this disagreement is the following. In Ref. 1 the individual opacities have been explicitly assumed as independent of the colliding hadrons and taken as Gaussians: $T_i(b) = (\sqrt{8\pi})^{-1} e^{-b^2/2a_i^2}$. However, one must keep in mind in doing so, that $T_i(b)$ cannot be chosen arbitrarily, and that it has to satisfy a normalization condition. Indeed, the two-dimensional integral of $T_i(b)$ over the impact parameter is just the three-dimensional integral over the density and it should then be normalized to a constant (generally taken as 1 or the product of the constituent numbers of the two hadrons, a consistent overall treatment leading anyway to the same result). Instead of that, the opacities of Ref. 1 lead to

$$(\sqrt{8\pi})^{-1} \int d^2\mathbf{b} e^{-b^2/2a_i^2} = \int d^3\mathbf{r} \rho(\mathbf{r}) = a_i^2 / \sqrt{2} .$$

These opacities then correspond to unphysical normalizations of the densities of the two hadrons. The g strength of Ref. 1, therefore, contains implicitly some geometrical dependence: namely, that which normalizes properly the densities. The single requirement of a correct density normalization, without any assumption on the hadronic constituents, leads to $g \approx g_0 / a_1^2 a_2^2$, and the conclusions of Ref. 1 can be reached only if the true interaction strength

g_0 satisfies the very strong constraint of compensating the geometry dependence (which is precisely that reported for σ_t) of this relation so as to keep g constant. Comparing with the present approach, where assumptions on the hadron constituents are made, it can be verified that one has $g \approx \sigma_0 A_1 A_2 / a_1^2 a_2^2$. For these reasons the geometry dependence reported in Ref. 1 is not correct, and this removes, with the above restriction on g_0 (or equivalently on σ_0), the formal grounds of the interpretation of σ_t , given in this reference.

Coming back to the present approach, note that, in the weak-absorption limit, $\chi(b)$ is small in relation (1); the exponential term can be expanded to first order, and the integral (1) appears just as the inverse Fourier transform of (2). One then recovers the usual impulse approximation

$$F(t) = A_1 A_2 G_1(t) G_2(t) f(t) \quad (5)$$

which leads straightforwardly to the additive quark model for the total cross section, consistently with relation (4). This relation, as the previous ones, can be easily generalized to the case of hadrons containing different quark flavors.

Concerning the slope of the forward cross sections, it is easy to see by means of relation (5) that the assumption of weak absorption and zero-range interaction leads to the same expression for the slope parameter as in Ref. 1: i.e., $B = a_1^2 + a_2^2$. However, relation (5) shows that the range of the interaction term may also contribute to the slope parameter, and that more realistic form factors, such as dipole or monopole expanded to first order in t , rather than Gaussians can be used. Finally, it is interesting to note that at the limit of weak absorption, when the geometrical dependence of the total cross section has vanished, the slope parameter remains the only scattering observable which can bring experimental information on the size of the interacting hadrons.

Experimentally known light-quark hadron systems, such as pp , $\bar{p}p$, or πp , exhibit some strong-absorption features since their opacities are large at small impact parameters.⁴ However, the "strong-absorption" terminology should not be taken as full absorption; the relative magnitudes of the elastic and inelastic cross sections in pp collisions, for example, are still far from the full absorption values (unitarity limit). Therefore, for these systems, the situation is intermediate between the limits discussed above. The amount by which the geometrical (strong-absorption) effects will affect the AQM limit can be estimated by developing relation (4) to the next-to-leading order,⁷ leading to

$$\sigma_t = A_1 A_2 \sigma_0 \left[1 - \frac{A_1 A_2 \sigma_0}{a_1^2 + a_2^2} \frac{1}{16\pi} \right] . \quad (6)$$

The first factor is the AQM limit, the second term in the parentheses corresponds to the fraction of σ_t depleted from the AQM limit by the opacity of the system, producing the geometrical dependence of σ_t .

At this point, one can attempt to account for the systematics of total cross sections¹ by means of relation (4), assuming σ_t to depend only on the hadron geometry: knowing the electromagnetic mean-square radius

(EMSR) of the proton, one can deduce the effective qq and $\bar{q}q$ cross sections from the σ_{pp} and $\sigma_{\bar{p}p}$ cross sections, by means of relation (4) (see Table I). Using the values obtained and assuming a Gaussian density for the pion (with¹⁶ $\langle r_\pi^2 \rangle = \text{EMSR} = 0.431 \text{ fm}^2$), one obtains $\sigma_{\pi^+p} = 27.4 \text{ mb}$ and $\sigma_{\pi^-p} = 28.1 \text{ mb}$. These values are markedly larger than the experimental values $\sigma_{\pi^+p}^{\text{expt}} = 23.4 \text{ mb}$ and $\sigma_{\pi^-p}^{\text{expt}} = 24 \text{ mb}$ (Ref. 17). The agreement is better for the pp system which has an equivalent constituent-quark content, and for which $\sigma_{pp}^{\text{expt}} \sim 26.7 \text{ mb}$ can be extracted from the photoproduction data at the same energy^{10,18} (see also Ref. 11). Therefore, the differences between σ_{pp} and $\sigma_{\pi p}$ or $\sigma_{\rho p}$ are approximately reproduced by relation (4), and appear to be partly geometrical indeed. The difference with the experimental values shows the limits of the approximations made: the dressing of the constituent-quark interaction should be somewhat different in baryon-baryon and in meson-baryon systems, because the population of other partons is different in a meson and in a baryon. This may result in different effective constituent cross sections. However, it must be noted that a better agreement would be obtained if the hadronic radius of the pion is smaller than its electromagnetic radius (dominated by the ρ -meson form factor), as suggested in Ref. 19. A better agreement is obtained with the simple AQM (Ref. 20); however, we believe that this is fortuitous, and that the present approach rests on better founded, and more consistent, physical grounds since it incorporates the effects of the hadronic opacity.

It is very interesting to turn next to systems which have different flavor contents such as ϕp and $J/\psi p$. For these systems, it can be easily verified that relation (4) cannot reproduce $\sigma_{\phi p}$ and $\sigma_{J/\psi p}$ using the value of σ_0 fitted to σ_{pp} and $\sigma_{\bar{p}p}$, the corresponding lower limit of relation (4) being $\sigma_{xp} \approx 25 \text{ mb}$ (with $a_x = 0$). This remarkable failure leads naturally to the assumption that the

TABLE I. Values of the imaginary part of the quark-quark effective amplitudes adjusted to the experimental σ_i for various hadronic systems at $\sqrt{s} \approx 16 \text{ GeV}$, using the analytical relation (4) as explained in the text. The values are given as effective cross sections $\sigma_{xq} = 4\pi \text{Im}f_{xq}(0)$. Here x stands for \bar{q} or q' [q' being any light quark (u, d) or antiquark different from \bar{q}], or S (strange quark or antiquark), or C (charmed quark or antiquark). The mean-square radius used for p (\bar{p}) is 0.648 fm^2 , other values are given in the text.

System	σ_i^{expt} (mb)	$\langle r_h^2 \rangle$ (fm^2)	σ_{xq} (mb)	x
pp	38.6 (Ref. 8)	0.648	5.23	q'
$p\bar{p}$	41.8 (Ref. 9)	0.648	6.22	\bar{q}
ϕp	12.1 (Refs. 10 and 11)	0.3 (Ref. 14)	2.2	S
$J/\psi p$	2.2 (Ref. 12, see also Ref. 13)	0.176 (Ref. 15)	0.38	C

effective qq interaction is flavor dependent. Table I gives the values of the effective cross sections $\sigma_{Qq} = 4\pi \text{Im}f_{Qq}(0)$ deduced for the Sq and Cq systems (S and C standing for either S or \bar{S} , and C or \bar{C} , respectively) from the experimental σ_i values, via relation (4), and using theoretical mean-square radii for the ϕ (Ref. 14), and the J/ψ (Ref. 15).

This strong flavor dependence of the inelasticity has been recognized some time ago²¹ in the interpretation of vector-meson photoproduction data, within the assumption of the vector-meson dominance of the photoproduction process.¹¹ It can be understood qualitatively in terms of the exchange mechanism governing the inelasticity of the interaction: a vector meson of given flavor will interact with a proton predominantly by exchanging mesons carrying the same flavor quantum number as the incident meson. The flavor dependence of the absorption has its origin in the mass of the mesons which can be exchanged between the two systems (charmed mesons are heavier than strange mesons, which are heavier than non-strange mesons), and thus in the mass of the exchanged quarks. These qualitative trends find a formal expression in the tensor dominance approximation of the Pomeron,^{21,22} which leads to a dependence of the vector-meson proton cross sections $\sigma_i(Vp) \approx m_V^{-2}$, m_V being the mass of the vector meson.

To end this section, we note that the application of the AQM rule to the σ_{xq} 's for the three systems, pp , ϕp , and $J/\psi p$, leads to an overestimate of the σ_i 's obtained with relation (4) or (6), amounting to 22%, 9%, and 3.5%, respectively. These numbers reflect the increasing transparency of the systems, and the corresponding increasing applicability of the AQM rule.

III. NUMERICAL APPROACH

We have further investigated this problem by numerical integration of relations (1) and (2). This allows us to use more realistic form factors (than Gaussians) for the interacting hadrons, and then to evaluate the sensitivity of the calculation to the form-factor assumptions. This approach leads to predictions for the differential cross section, which compared to experimental data is more constraining than the single σ_i values. The eikonal relations (1) and (2) have been used to fit pp and $p\bar{p}$ elastic-scattering data, by adjusting the parameters σ_{qq} , $\alpha = \text{Re}f(0)/\text{Im}f(0)$, a , b , and c , of the phenomenological qq effective amplitude used in Refs. 5 and 23:

$$f_{qq}(t) = \frac{\sigma_{qq}}{4\pi} (i + \alpha)(1 + at)^{-1/2} e^{i(b|t| + ct^2)}. \quad (7)$$

Note the slightly different definition used here (the values given for the parameter K in Ref. 5, must be divided by 4π for consistency with the definition). A detailed account of the complete analysis of experimental data will be given elsewhere. Consistent results are obtained from fitting the pp data over the CERN ISR energy range. Figure 1 shows a sample of the fits obtained at several energies for pp and $p\bar{p}$, using the parametrization of Ref. 24 to describe the proton form factor. Similar results are obtained with the parametrization of Ref. 25,

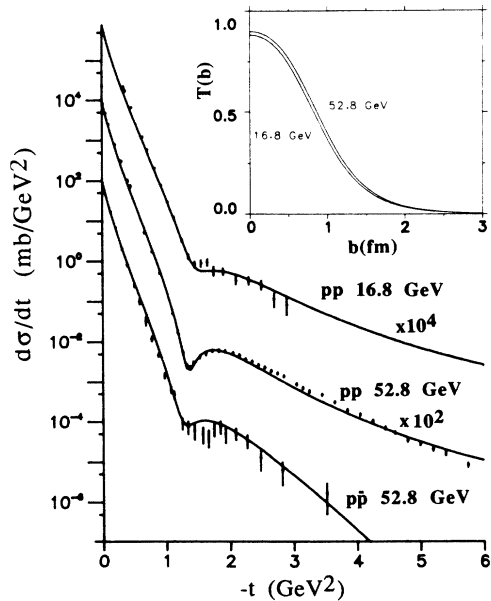


FIG. 1. Sample of fits obtained on high-energy pp and $p\bar{p}$ data (Refs. 10 and 16) as described in the text. The inset shows the opacity function for the pp system at $\sqrt{s} = 16.8$ and 52.8 GeV.

but no good result could be obtained with usual dipole shape (which gives a poor description of the experimental electromagnetic form factor at large- t values). For the energy of interest here, the values obtained are $\alpha, a, b, c = -0.08, 0.06, 0.18, -0.1$, and $0.18, 0.1, 0, 0$ for f_{qq} and $f_{\bar{q}q}$, respectively (see Table II for the other parameters). The inset in Fig. 1 shows the calculated opacity (inelastic) function $T(b) = 1 - |e^{-\chi(b)}|^2$ for pp at $\sqrt{s} = 52.8$ GeV. Note the large absorption observed in the central region (in agreement with Ref. 26) which generates the geometrical dependence of σ_t , as discussed in the previous section. It must also be pointed out that the calculated total cross sections obtained from fits to the differential cross section for pp and $p\bar{p}$ are in good agreement with the experimental values. This is obtained by virtue of the phase parameter in the effective amplitude.²³ Setting this parameter to zero would lead to overestimating the experimental values by about 10%.

A mean to probe the consistency of the present ap-

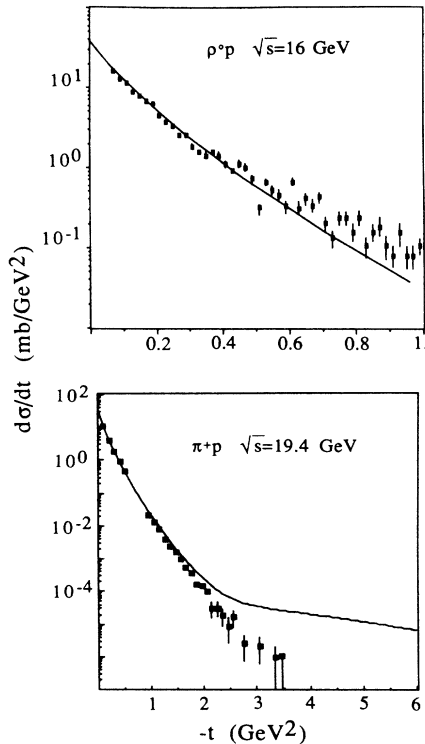


FIG. 2. Calculated cross sections for πp at $s^{1/2} \approx 19.4$ GeV and ρp at $s^{1/2} \approx 9.2-11.9$ GeV, compared to the experimental data (Refs. 27 and 29). The calculations have been done with the effective interaction parameters fitted to the pp and $p\bar{p}$ data (see text).

proach is to test its ability to reproduce the cross section of other systems. The above values of the parameters have been used to calculate the πp cross section at 200 GeV laboratory energy.²⁷ The results are shown on Fig. 2. The agreement with the data is excellent over the range $0.1 < -t < 2$ GeV². A fit of the amplitudes on these data leads to a hardly better result, indicating that the increasing disagreement at larger $-t$ is more due to the pion form factor²⁸ than to a lack of consistency of the approach at large $-t$. Figure 2 also shows that an equivalent agreement is obtained for the ρp system at 45–75 GeV (Ref. 29). We emphasize that no parameter has been adjusted in these latter calculations. This

TABLE II. Same qq effective cross sections as in Table I, obtained by numerical integration as discussed in the text. The experimental and calculated forward angle slope parameters (at $t = -0.2$ GeV² for pp and $p\bar{p}$) of the differential cross sections are also given (see Table I for experimental references).

System	σ_t^{expt} (mb)	B^{expt} (GeV ⁻²)	σ_t^{calc} (mb)	B^{calc} (GeV ⁻²)	σ_{xq} (mb)	x
pp	38.6	10.25	39.4	10.77	5.33	q'
$p\bar{p}$	41.8	10.97	41.8	11.1	6.05	\bar{q}
ϕp	12.1	6.7		8.1	2.2	S
$J/\psi p$	2.2	5.2		6.05	0.38	C

demonstrates that the present phenomenological approach is able to account consistently and quantitatively for the differential cross section of hadronic systems containing only light (u, d) quarks, at least up to $-t \approx 1.5-2$ GeV^2 . It allows us to further conclude that the (phenomenological) dynamical content of the model is satisfactory over this range.

For the ϕp and $J/\psi p$ systems, the experimental σ_i values have been used to adjust the effective constituent cross section using the same procedure as previously. The matter distribution in the meson is described with a usual monopole propagator-type shape:^{8,12} $G(t)=(1+t/\mu^2)^{-1}$, the μ parameter being of the order of the meson mass (see Ref. 30 for the theoretical grounds of this shape). In the following, we have used $\mu_\phi^2=1.04$ GeV^2 , and $\mu_{J/\psi}^2=9.6$ GeV^2 . Figure 3 shows the calculated angular distributions for the ϕp and $J/\psi p$ systems. For the two calculations, the σ_{qq} parameter has been adjusted empirically so as to fit the calculated σ_i on the experimental value. In these calculations, the weak t dependence for $f_{q'q}(t)$ ($a=0.06$), fitted on pp has been conserved. However, taking $a=0$ does not appreciably change the results. Taking α constant is also a questionable approximation. However, α is expected to be small (and has been found small experimentally¹³), even for the more weakly absorbing system, and the uncertainty on its precise value does not affect the conclusion of the present analysis (see Ref. 31 on the flavor dependence of α). The inset shows the opacity functions obtained for the two systems. One observes, as it was anticipated in the Introduction, that the opacity decreases with the mass of the constituent quarks of the incident meson.

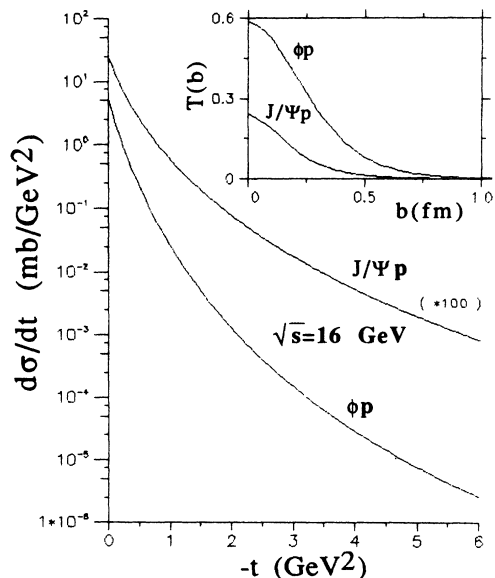


FIG. 3. Cross sections and opacities calculated with the model of Refs. 5 and 23 for the systems ϕp and $J/\psi p$, with the effective interaction adjusted so as to reproduce the experimental total cross section, as explained in the text.

Table II gives the effective quark-quark cross section σ_{Qq} fitted to the data. Comparison with Table I shows that the results obtained numerically are quite close to those obtained by means of the analytical relation (4). This consistency of the two approaches is very satisfactory and provides a sounder basis to the analytic model of the previous section. It must be noted that the form factors used to describe the ϕ and J/ψ correspond to mean-square radii markedly smaller than theoretically predicted.^{14,15} However, for these projectiles, the influence of the geometry is weak (see Sec. II), and the use of form factors consistent with the theoretical MSR's leads to results differing by less than 5% from those given in the table. In this case, the precise shape of the meson form factor has little effect on the values of σ_i , which is essentially determined by the AQM rule. The slope parameters $B=(d/dt)\ln(d\sigma/dt)$ obtained in the calculations are also given. The agreement with the experimental values is not very good for the heavy-flavor projectiles. However the trend of the experimental slopes to decrease with the increasing mass of the incident quarks is qualitatively reproduced, providing further indications of the correctness of this approach.

Figure 4 shows the three values obtained for σ_{xq} , plotted as a function of the inverse constituent-quark mass of the (projectile) hadron. This representation is suggested by the success of the tensor-dominance model of the Pomeron.^{21,22} The three points line up quite nicely in logarithmic coordinates, exhibiting a power-law dependence. They can be fitted with a functional form $\sigma_{xq}=\alpha m_x^{-\beta}$, with $\alpha=0.73\pm 0.05$ and $\beta=1.63\pm 0.05$. The error bars reflect the uncertainty on the constituent-quark masses. The exponent is smaller than would be expected from the tensor-dominance approximation which predicts a m_V^{-2} dependence for the total cross section. Extrapolating this empirical law to the constituent mass of the b quark ($m_b \approx 5$ GeV) leads to a value of $\sigma_{bq} \approx 55$

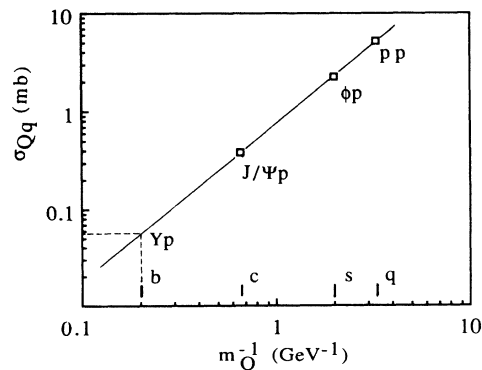


FIG. 4. Effective quark-quark cross sections σ_{xq} obtained from the phenomenological analysis described in the text, plotted as a function of the inverse constituent-quark mass of the projectile hadron ($m_q \approx 0.3$ GeV , $m_s \approx 0.5$ GeV , $m_c \approx 1.5$ GeV). The labeling of the points indicates the system from which the σ_{xq} value has been extracted. The dashed line is a fit with the functional form $\sigma_{xq}=0.73m_q^{-1.63}$ in the units of the figure.

μb , and thus to an estimate of the total cross section for the Υp system $\sigma_{\Upsilon p} \approx 330 \mu\text{b}$. For this system, the AQM rule gives an agreement better than 1% with the numerical calculation. The value obtained is situated within the range covered by the predictions obtained from the above-quoted dependence on m_V^{-2} , using the σ_{pp} value ($\sigma_{\Upsilon p} \approx 170 \mu\text{b}$), and some more refined predictions, also based on the tensor dominance of the Pomeron ($\sigma_{\Upsilon p} \approx 400 \mu\text{b}$) (Ref. 32).

The spirit of the theoretical framework used in the present analysis is the same as that of the valon model,³³ and the effective constituent cross sections obtained here can be identified to valon-valon cross sections. The constituents, or valons, are composite objects, constituted of a valence (current) quark surrounded with its cloud of (bremsstrahlung) gluons and sea-quark pairs. They have some size and their spatial extent can be described with a form factor.³⁴ Their universal structure arises from QCD elementary virtual processes. We have seen above that the constituent cross sections obtained depend on the constituent mass in a way reminiscent of the tensor dominance of the Pomeron. This is in qualitative agreement with Ref. 35 where it is argued that the Regge behavior of nucleon structure derives from the Regge behavior of its constituents. These results are also consistent with the assumption of direct coupling of the Pomeron to individual quarks in hadrons.³⁶ Note, however, that in Ref. 36, this assumption is based on the success of the AQM to account for σ_t in systems such as $pp, \pi p$. This is a questionable argument in account of the present analysis.

IV. SUMMARY AND CONCLUSION

In conclusion, we have seen that, in a simple eikonal approach using Gaussian densities, the total hadronic

cross sections do exhibit some geometrical dependence when the absorption is strong. However, the systems remain dominated by the interaction term of the AQM. When the absorption weakens, the geometrical dependence fades away and total cross sections are then described by the additive quark model at the limit of vanishing absorption. The (moderately) strong-absorption (geometrical) case applies to the $pp, \bar{p}p$, and πp systems, whereas the ϕp and $J/\psi p$ systems fall closer to the weak-absorption (AQM) limit. These conclusions are based on the single assumption that diffractive elastic scattering of hadrons originates from the shadow of the opacity created by inelastic processes. The large variations of the experimental total cross sections observed in Vp systems (V is the vector meson) can be consistently understood in terms of the dynamics of the inelasticity and its dependence on the flavor of the vector-meson constituents, and not at all by the hadronic geometry. It can be accounted for by means of an effective interaction f_{qq} , incorporated into the Glauber formalism, and fitted to the data. The model then acquires some predictive power, and may serve as a guide line for experimental projects. It is being used to predict hyperon-nucleon cross sections in the prospect of experiment WA89 at CERN.

ACKNOWLEDGMENTS

The authors are grateful to C. Gignoux, M. Giffon, J. M. Richard, J. Soffer, and C. Wilkin for helpful discussions and critical reading of the manuscript.

¹B. Povh and J. Hufner, Phys. Rev. Lett. **58**, 1612 (1987).

²P. J. Karol, Phys. Rev. C **11**, 1203 (1975).

³S. Kox *et al.*, Phys. Rev. C **35**, 1678 (1987).

⁴For recent reviews, see L. L. Jencovsky, Riv. Nuovo Cimento **10**, 1 (1987); R. Castaldi and G. Sanguinetti, Annu. Rev. Nucl. Part. Sci. **35**, 351 (1985); G. Alberi and G. Goggi, Phys. Rep. **74**, 1 (1981).

⁵R. J. Glauber and J. Velasco, Phys. Lett. **147B**, 380 (1984).

⁶J. Y. Hostachy *et al.*, Phys. Lett. B **184**, 139 (1987); R. de Vries and J. C. Peng, Phys. Rev. C **22**, 1055 (1980).

⁷M. Abramowitz and I. A. Stegun, *Handbook of Mathematical Functions* (Dover, New York, 1965), p. 229.

⁸A. Schiz *et al.*, Phys. Rev. D **24**, 26 (1981); L. A. Fajardo *et al.*, *ibid.* **24**, 46 (1981).

⁹K. R. Schubert, *Nuclear and Particle Physics*, (Landolt-Bornstein, Vol. 9a) (Springer, Berlin, 1980), p. 216.

¹⁰R. M. Eglhoff *et al.*, Phys. Rev. Lett. **43**, 657 (1979); R. M. Eglhoff, Ph.D. thesis, University of Toronto, 1979. See also R. L. Anderson *et al.*, Phys. Rev. D **4**, 3245 (1971).

¹¹T. H. Bauer, R. D. Spital, D. R. Yennie, and F. M. Pipkin, Rev. Mod. Phys. **50**, 261 (1978); for recent results on the validity of the VDM, see J. J. Aubert *et al.*, Phys. Lett. **161B**, 203 (1985).

¹²J. J. Aubert *et al.*, Nucl. Phys. **B213**, 1 (1983).

¹³S. D. Holmes, W. Lee, and J. E. Wiss, Annu. Rev. Nucl. Part.

Sci. **35**, 39 (1985).

¹⁴J. L. Basdevant and S. Boukraa, Ann. Phys. (Leipzig) **10**, 475 (1985).

¹⁵W. Buchmuller and S-H. H. Tye, Phys. Rev. D **24**, 132 (1981).

¹⁶S. R. Amendolia *et al.*, Nucl. Phys. **B277**, 168 (1986).

¹⁷D. S. Ayres *et al.*, Phys. Rev. D **15**, 3105 (1977).

¹⁸P. Roudeau, thesis, Université d'Orsay, Report No. LAL-80/14, 1980.

¹⁹G. E. Brown, M. Rho, and W. Weise, Nucl. Phys. **A454**, 669 (1986).

²⁰B. Margolis, Nucl. Phys. **B6**, 687 (1968).

²¹C. E. Carlson and P. G. O. Freund, Phys. Rev. D **11**, 2453 (1975).

²²R. Carlitz, M. B. Green, and A. Zee, Phys. Rev. D **4**, 3439 (1971).

²³R. J. Glauber and J. Velasco, in *Proceedings of the 2nd International Conference on Elastic and Diffractive Scattering*, New York, New York, 1987, edited by K. Goulianos (Editions Frontières, Gif-sur-Yvette, France, 1988).

²⁴F. Borkowski *et al.*, Nucl. Phys. **B93**, 461 (1975).

²⁵R. Felst, DESY Report No. 73-56, 1973 (unpublished).

²⁶U. Amaldi and K. R. Schubert, Nucl. Phys. **B166**, 301 (1980).

²⁷R. Rubinstein *et al.*, Phys. Rev. D **30**, 1413 (1984).

²⁸C. H. Lai, S. Y. Lo, and K. K. Phua, Phys. Lett. **122B**, 177 (1983); C. Bourrely, P. Chiappetta, J. Soffer, and T. T. Wu,

- ibid.* **132B**, 191 (1983).
- ²⁹D. Aston *et al.*, Nucl. Phys. **B209**, 56 (1982).
- ³⁰L. G. Lansberg, Phys. Rep. **128**, 301 (1985).
- ³¹D. Horn, Phys. Lett. **73B**, 199 (1978).
- ³²N. E. Bralic, Nucl. Phys. **B139**, 433 (1978).
- ³³R. C. Hwa, Phys. Rev. D **22**, 759 (1980); R. C. Hwa and S. Zahir, *ibid.* **23**, 2539 (1981).
- ³⁴R. C. Hwa and C. S. Lam, Phys. Rev. D **26**, 2338 (1982).
- ³⁵G. Altarelli, N. Cabibbo, L. Maiani, and R. Petronzio, Nucl. Phys. **B69**, 531 (1974).
- ³⁶A. Donnachie and P. V. Landshoff, Phys. Lett. B **191**, 309 (1987); Nucl. Phys. **B267**, 690 (1986).